Journal of Electrical Engineering, Vol. 75, No. 4, 2024, pp. 317-324

sciendo

PAPERS

Series partial power converter with half bridge LLC series resonant converter for PV application

Sebin Davis Kurichiparambil, Varghese Jegathesan

This study proposes a series partial power converter with a half-bridge LLC series resonant converter for photovoltaic (PV) applications. The main advantage of the implementation of a partial power converter with LLC series resonant converter is zero voltage switching (ZVS) operation of primary side enables the converter to work at a higher switching frequency. The partial power topology used in the proposed converter enables low power rating switches in the primary, which in other terms reduces the primary current. The proposed converter achieves excellent efficiency due to its ZVS and partial power operating capabilities. The valuation of the proposed converter is done in MATLAB Simulink with a 300 W PV module, which is made to operate in varying irradiance and module temperature of 25 °C. The operational waveforms and the power outputs obtained when the proposed converter is implemented by using perturbation and observation (P&O) maximum power point tracking (MPPT) control algorithm are discussed in this paper.

Keywords: LLC series resonant converter, partial power converter, PV applications, MPPT, DC-DC converters

1 Introduction

Renewable energy systems, such as photovoltaic (PV) and wind power systems, are rapidly developing to overcome the challenge of global climate change and aid sustainable environmental development. Better efficiency, higher power density, and higher reliability are now in focus in power supply design and application. PV systems are more promising as a distributed power source due to their modular design properties and simplicity of installation, as well as their ability to be located closer to the load side. PV power extraction from PV Module, MPPT, voltage level shifting, and current-controlled power injection to the grid is different tasks to be executed by a grid-connected inverter. All of these functions must be addressed by a single converter in single-stage topologies which makes single-stage inverter control complex and reduced system efficiency [1]. In order to overcome the drawbacks two-stage topologies are preferred [2, 3]. A two-stage grid-tied photovoltaic (PV) system consists of PV array, a DC/DC converter stage, and a DC/AC converter stage[4]. Researchers are focusing their efforts on developing high-efficiency, low-cost power sources by upgrading current topologies and algorithms.

Performance of the PV power generating system is mainly decided by efficiency of DC/DC converter, which is performing MPPT. When transitions in switched-mode DC/DC converters are Hard-switched, the result will be substantial power losses, which reduces converter efficiency and increasing the risk of switching device breakage [5]. Among the several control techniques used in DC-DC converters, partial power processing (PPP) offers benefits such as reduced cost and higher power density with a reduced power rating of converters [6]. Along with improving the efficiency of PV conversion modules, there are continuous attempts to reduce volume and size by increasing the switching frequency. This research proposes a Series Connected Partial Power converter (S-PPC) architecture which will maximise the efficiency of the DC/DC converter. S-PPC improves its efficiency by transferring a major portion of power to the load directly unprocessed [7]. S-PPC processes a small portion of power to attain MPPT performance of DC/DC stage [8]. An isolated DC/DC converter is required for S-PPC converter, as a basic circuit component and it is modified to work. In DC-DC converters, partial power processing may be implemented by connecting the input and load in series or connecting the output and the power source in series [9].

High-frequency (HF) transformer based resonant converters can provide a better efficiency over a broad range of loads and provide galvanic isolation, making them ideal for PPC topologies. The main two types of resonant converters are two elements and three elements resonant [10]. Poor voltage regulation in light load conditions and a very low range of zero voltage switching are disadvantages of the two-element resonant arrangement (ZVS) [11]. Figures 1a and 1b show the two basic types of two-element resonant converter topologies [12] implemented using half-bridge topology.

Department of Electrical and Electronics Engineering, Karunya Institute of Technology and Sciences, Tamil Nadu, India
sebindavisk@gmail.com

https://doi.org/10.2478/jee-2024-0038, Print (till 2015) ISSN 1335-3632, On-line ISSN 1339-309X

When considering the element resonant converter, one circuit uses one inductor and two capacitors called as LCC configuration. The LCC resonant converter requires a large-sized capacitor which will be expensive due to high AC currents [13]. Two inductors and one capacitor can reproduce the same characteristics forming an LLC configuration [14]. The ZVS as well as zero current switching (ZCS) of the LLC resonant converter ensures high conversion efficiency [15]. The circuit diagram for implementing LLC and LCC configuration of the resonant converter with half-bridge (HB) topology is shown in Figs. 2a and 2b. Comparing the cost and efficiency the HB LLC converter is selected for the implementation of S-PPC [16] via pulse width modulation. The switching frequency of resonant converter is changed in order to regulate the output voltage [17]. Compared to hard switched DC/DC topology the soft switched resonant converters process with higher efficiency and the presence of galvanic isolation makes the HB LLC converter best to use with S-PPC topology [18, 19]. Power switches may be used in zero-voltage switching (ZVS) because the LLC series resonant converter inherits inductive function [20]. Zero-current switching (ZCS) is attained by rectifier diodes when applied switching frequency is below resonant frequency of resonant inductor and capacitor [21]. Switching losses of LLC resonant converter is reduced by ZCS and ZVS switching [22].

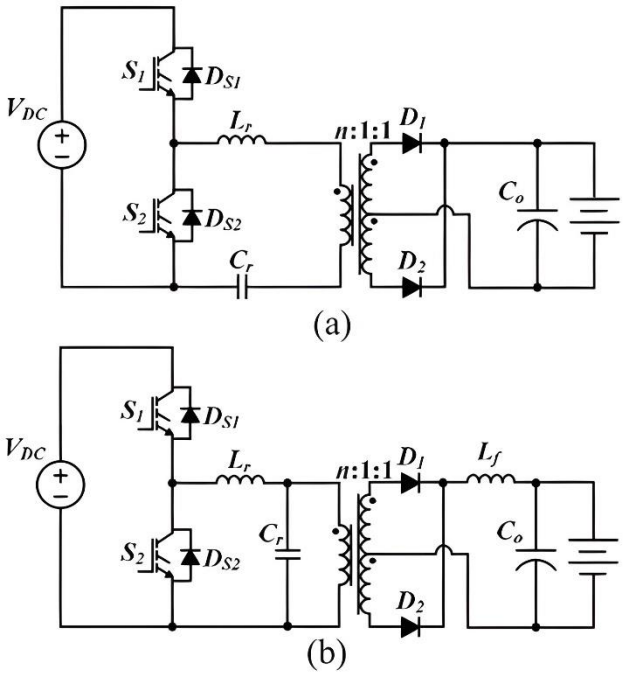

Fig. 1. Two element resonant topologies: (a) Series resonant converter (SRC), (b) parallel resonant converter

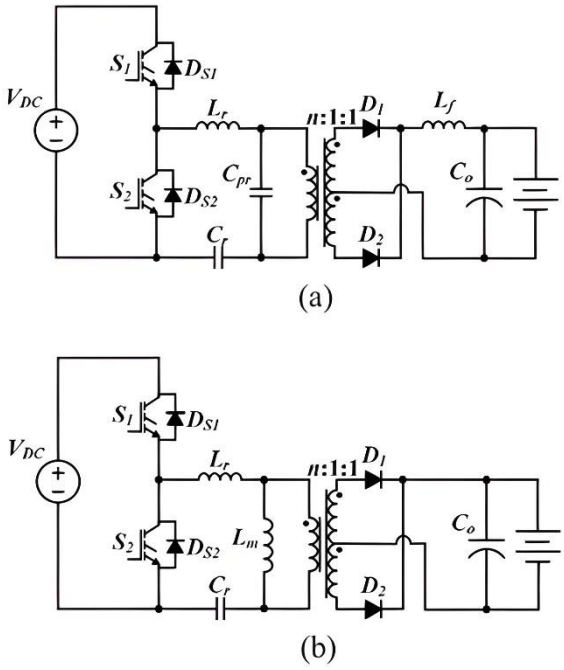

Fig. 2. Two element resonant topologies: (a) LCC series-parallel resonant converter, (b) LLC series-parallel resonant converter

This paper is organized as follows. Section 2 discusses the proposed converter along with the analysis of the converter. Section 2 consists of 3 subsections. It includes detailed discussion on the proposed topology, control strategy proposed for the converter and its design. The simulation results shown in section 3 evaluate the performance of the proposed converter. Conclusion is discussed in section 4.

2 Series connected PPC-based DC-DC converter for PV system

The major application of S-PPC topology DC/DC converters is in the PV optimizers, in which the input of converter is connected to PV module and the output is connected serially forming a high voltage DC bus. The PV optimizer's duty to make sure that each PV module's operating point is at maximum power point (MPP) and to eliminate losses caused by partial shadowing and PV module mismatch [23]. The main function of a string inverter when used with a PV optimizer is to keep the DC bus voltage constant while sending energy to the grid. The same topology also can be implemented as the first stage of the microinverter. The proposed topology is making use of the S-PPC topology implemented with HB LLC with perturb and observe (P&O) MPPT algorithm.

2.1 Conventional isolated series LLC half-bridge resonant converter

ZVS mode of switching for the primary-side switches and ZCS mode of switching for the secondary-side rectifiers might be achieved using an isolated LLC resonant converter shown in Fig. 2b. To find out the voltage gain formula, circuit model shown in Fig. 3 based on the Fundamental Harmonic Approximation (FHA) is used [24].

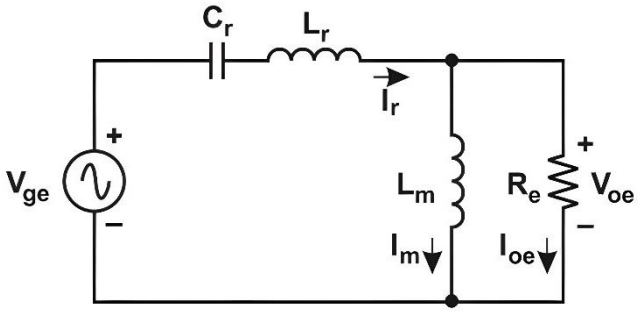

Fig. 3. Linear sinusoidal circuit model of LLC resonant half-bridge converter

The fundamental component of the switch node voltage is represented by V_{ge}. The fundamental component in secondary side bipolar square-wave voltage is represented by V_{oe}. The approximate linear circuit with input as sinusoidal input source with equivalent resistive load. The ratio of the input voltage to the output voltage of the converter can be represented by M_{g-DC}. While considering approximation using fundamental components, voltage ratio can be found and is represented by M_{g-AC}.

$$M_{g-DC} = \frac{n\,V_0}{V_{in}/2} = \frac{n\,V_0}{V_{DC}/2} \tag{1}$$

Equation (1) may be approximated by taking ratio of the bipolar square-wave voltage the unipolar square-wave voltage. In the same way the AC voltage ratio can be represented as a ratio of fundamental component V_{ge} and V_{oe}.

$$M_{g-DC} = \frac{V_{oe}}{V_{ge}} \tag{2}$$

M_{g-AC} can be generally represented as converter gain M_g and it can be expressed as the relation between circuit parameters L_r, L_m, C_r, and R_e.

$$M_g = \left| \frac{j\omega L_m || R_e}{j\omega L_m || (R_e + j\omega L_r + \frac{1}{j\omega C_r})} \right| \tag{3}$$

Equation (3) helps to find the relation between input voltage V_{in} output voltage V_0. Considering the aspect of approximation, V_0 can be represented as

$$V_0 = M_g \cdot \frac{1}{n} \cdot \frac{V_{in}}{2}. \tag{4}$$

In order to simplify the gain formula normalized parameters are applied to Eqn. (3). The resonant frequency f_0 is selected for normalising frequency. The normalized frequency f_n is represented as a ratio of switching frequency f_{sw} to the resonant frequency f_n.

$$f_n = \frac{f_{sw}}{f_0} \tag{5}$$

The two inductors present in the circuit can be combined from one normalised inductor L_n and can be represented as

$$L_n = \frac{L_m}{L_r}\,. \tag{6}$$

The quality factor of the proposed resonant circuit represented by Q_e is defined as

$$Q_e = \frac{\sqrt{L_r/C_r}}{R_e}\,. \tag{7}$$

Applying Eqns. (5-7) in Eqn. (3), the normalised gain can be expressed as

$$M_g = \left| \frac{L_n f_n^2}{(L_n+1)f_n^2 - 1 + j(f_n^2-1)f_n Q_e L_n} \right|. \tag{8}$$

The typical response of voltage gain function M_g towards the normal frequency is shown in Fig. 4. It can be noticed that when L_n is fixed and the Q_e value is reduced, the frequency control band in getting reduced.

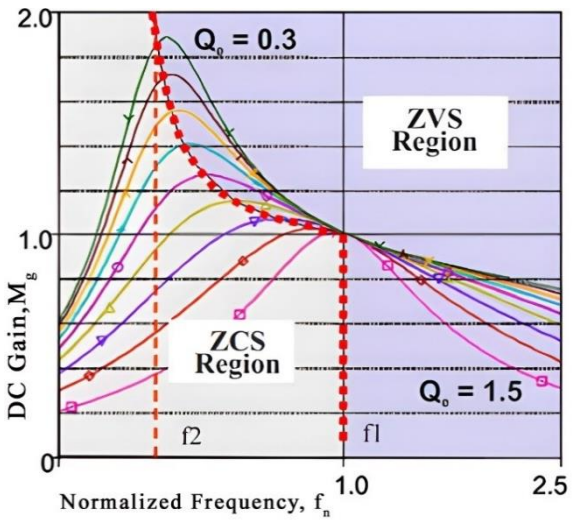

Fig. 4. Normalized gain versus frequency waveform of LLC resonant converter

The switching losses of the converter may be greatly minimised by ensuring that the primary side ZVS is maintained throughout the working range. The MOSFET is turned on only after its source voltage has been reduced to zero by external means to achieve ZVS. Only when the converter's input phase angle is larger than zero, which may be acquired by input impedance inductive, can ZVS be accomplished. But when operated in a capacitive region ZVS cannot be achieved, which makes the converter switching losses high. The working range of this converter is set above resonance frequency to assure ZVS performance.

When analysing the curves in Fig. 4, the range of switching frequency to attain ZVS and ZCS can be estimated. The converter operates in ZVS mode when switching frequency is greater than f_1. The converter operates at ZCS conditions at all operating points when the switching frequency is less than f_2. The amount load in converter decides whether the converter operation is at ZVS or ZCS while switching frequency is between f_1 and f_2.

$$f_1 = \frac{1}{2\pi\sqrt{L_r C_r}} \tag{9}$$

$$f_2 \frac{1}{2\pi\sqrt{(L_r + L_m)C_r}} \tag{10}$$

2.2 S-PPC topology LLC half-bridge resonant converter

Figure 5 shows the proposed S-PPC converter with HB-LLC topology. The proposed S-PPC converter structure is mainly composed of an isolated DC/DC converter (here an HB series LLC resonant converter is used) whose input is connected in series with secondary side, and output is connected in parallel to main side. The MPPT is implemented by varying the switching frequency in the range such that the converter is working in the ZCS region. The voltage gain of proposed converter is derived by applying Kirchoff laws to the S-PPC shown in Fig. 5.

$$V_{dc} = V_{pv} + V_{conv} \tag{11}$$

$$I_{in} = I_{conv} + V_{out} \tag{12}$$

The fraction of the active power processed by converter to total DC-DC stage input power can be termed as partial power ratio K_{pr}.

$$K_{pr} = \frac{V_{pv}\, I_{conv}}{V_{pv}\, I_{in}} \tag{13}$$

By applying Eqn. (12) to (13)

$$K_{pr} = 1 - \frac{I_{out}}{I_{in}} \tag{14}$$

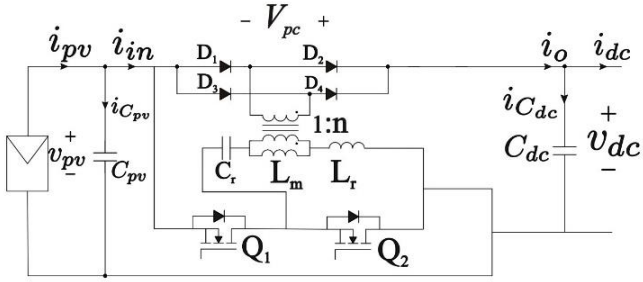

Fig. 5. Schematic diagram of the proposed HB LLC series resonant converter with S-PPC configuration

Considering ideal components, the efficiency of the DC-DC stage can be written as

$$\eta_{dc} = \frac{V_{dc}\, I_{out}}{V_{pv}\, I_{in}}, \tag{15}$$

$$\eta_{dc} = G_v \frac{I_{out}}{I_{in}}. \tag{16}$$

G_v denotes the DC-DC stage voltage gain ratio. The partial power ratio K_{pr} may be written as a function of DC stage efficiency and voltage gain:

$$K_{pr} = 1 - \frac{\eta_{dc}}{G_v}. \tag{17}$$

The voltage gain obtained by HB-LLC series resonant converter used can be written as

$$G_{conv} = \frac{M_g}{2n}. \tag{18}$$

Applying (11) to (18), the voltage gain of the proposed converter can be written as

$$\frac{V_{dc} - V_{pv}}{V_{pv}} = \frac{M_g}{2n}. \tag{19}$$

Rearranging Eqn. (19) to find the DC-DC converter stage voltage gain termed as global gain, G_v can be written as

$$G_v = 1 + \frac{M_g}{2n}. \tag{20}$$

2.3 Control scheme of the proposed system

The control algorithm for tracking MPPT performs by varying the frequency in a range in such a way that it is ensuring the ZCS and ZVS operation of the converter. The output voltage V_{dc} of the PPC converter is regulated in the same way that the Q1 and Q2 switches are adjusted in a typical LLC series resonant converter. Changing the switching frequency to attain the needed maximum power point is how MPPT tracking is accomplished. The conventional P&O MPPT algorithm is modified to

accommodate the proposed topology. The flowchart of control scheme, the suggested for the topology is shown in Fig. 6. In the suggested method, the panel voltage $V$is varied. The voltage and current at the PV terminals are sensed, measured, and used to examine the performance of the produced power. The algorithm is designed in such a way that the change in the frequency is in the allowable range as per the resonant component design and accommodates the ZCS and ZVS switching properties.

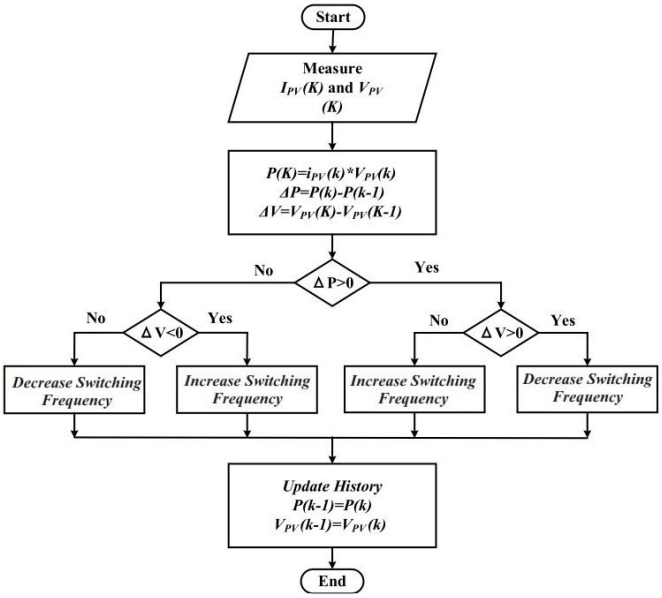

Fig. 6. Control scheme of the proposed converter

The control scheme is developed by applying the P&O algorithm by switching frequency to change to track MPPT. When a reduction in switching frequency is applied, the LLC series resonant converter output voltage rises. For maintaining the ZVS and ZCS modes of operation, the switching frequency band is set as a maximum of 120 kHz and a minimum of 80 kHz. The P&O approach modifies the converter's output by varying the switching frequency. While considering the proposed converter, the S-PPC topology enables the designer to reduce converter rating as the LLC series resonant converter only needs to process a portion of the total power as per Eqn. (13). In the proposed control, $I_{pv}(k)$ and $V_{pv}(k)$ are the current values of PV module current and voltage, and $V_{pv}(k–1)$ and $I_{pv}(k–1)$ are PV voltage and PV current of the previous sampling. The voltage is perturbed by introducing a small change in the switching frequency and generated power behaviour is then examined. Based on this analysis, the decision is made on increasing or decreasing the switching frequency.

3 Simulation results and analysis

The proposed model was simulated in MATLAB SIMULINK platform using parameters shown in Tab. 1 in order to validate the validity of proposed LLC resonant DC-DC converter design within applicable operating frequency. Table 2 shows the parameter values for the 300W PV module utilised in the simulation.

Table 1. The LLC resonant tank parameters

Parameter	Value
Resonant capacitor	470 nF
Resonant inductor	5.4 µH
Magnetizing inductor	14.2 µH
Resonant frequency	100 kHz
Operating range	80 kHz – 120 kHz

Table 2. PV module parameters

V_{mp} (V)	I_{mp} (A)	MPP (W)	I_{SC} (A)	V_{OC} (V)
35	8.57	315	9.3	43

As per Eqn. (20), when the transformer turns ratio is high, a small change in the switching frequency applied, a very large change in gain is produced. So, the turns ratio of 1:1 is used in the simulation to avoid the requirement of a highly precise control algorithm. Different irradiance levels of 1000, 900, 800, and 600 W/m^2 are applied to check the effectiveness of the proposed topology.

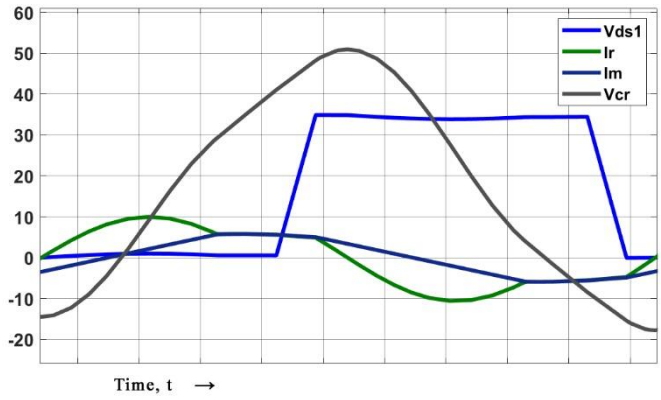

Fig. 7. One switching cycle operation waveforms of the proposed converter while 1000 W/m^2 irradiance is applied to the PV module

The operational waveforms formed for one sample cycle are shown in Fig. 7 and are obtained when a 1000 W/m^2 irradiance level is applied to the PV module. When 1000 W/m^2 is applied, the control algorithm tracks the switching frequency to 118 kHz. Since the resonant current lags behind the half-bridge voltage on the primary side MOSFET voltage, primary-side MOSFETs are achieving ZVS mode upon turning on. Figure 8 indicates current drops to zero before the first half-cycle ends, shown in the positive half cycle, and diodes D2 and D3 conduct in the negative half cycle.

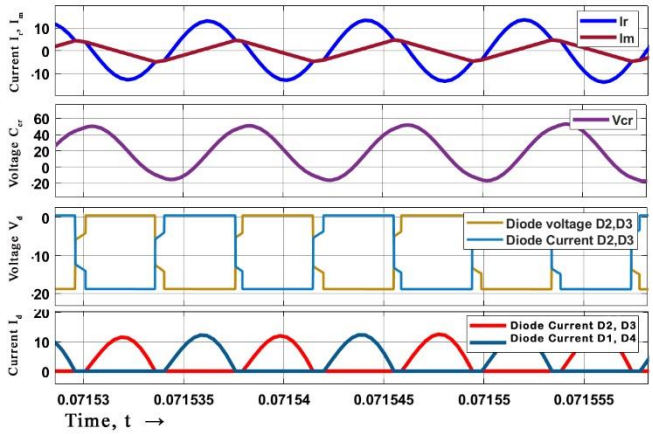

Fig. 8. Simulation waveforms at MPP showing primary side and secondary side components at irradiance level of 900 W/m^2

To verify the effectiveness of the MPPT control technique with the proposed HB-LLC S-PPC topology, varying irradiance is applied. The operational waveforms obtained when different irradiance levels are applied are shown in Fig. 8. When 1000 W/m^2 irradiance level is applied, the switching frequency applied was 105 kHz and the maximum efficiency of the converter was 99.2%. Then the percentage partial power ratio K_{pr} was 33%, which indicates the portion of total power which is processed by the converter. When irradiance varies from 1000 to 600 W/m^2, the switching frequency varies to 118 kHz and the efficiency of 96.3% is maintained by varying K_{pr} to 33%. The operational waveforms of the converter with irradiance levels of 1000, 900, 800 and 600 W/m^2 are shown in Fig. 9. The power processed by the proposed converter is shown as P_{conv} and it can be observed that only a portion of total power P_{out} is processed by the converter. By comparing the PV power P_{pv} and output power P_{out}, efficiency of up to 99.2% is achieved under 1000 W/m^2 irradiance. Even in the situations, when the converter is processing a higher resonant current, the converter performs ZVS mode operation on the primary-side and ZCS mode of operation on the secondary-side at higher irradiance levels.

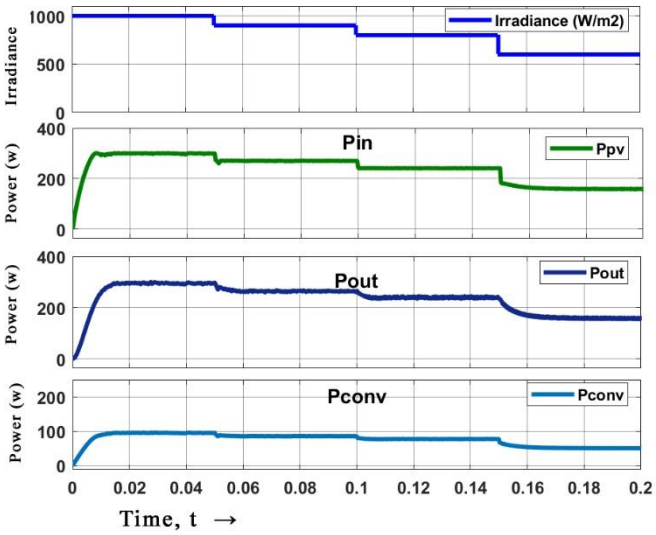

Fig. 9. Performance of proposed S-PPC for different irradiance levels

The proposed converter operation efficiency is compared with other converters when applied with P&O MPPT algorithm and variable irradiance is plotted in Fig. 10. The low switching loss due to the ZVS and ZCS operation of the proposed converter helps it to dominate in output efficiency. When applied with 1000 W/m^2 irradiance, a conventional flyback converter exhibits 94.6% efficiency, flyback PPC 96.2% efficiency, full bridge PPC 97.2% efficiency and the proposed converter is 99.2%. The soft switching capability of the proposed converter allows to perform in very high efficiency.

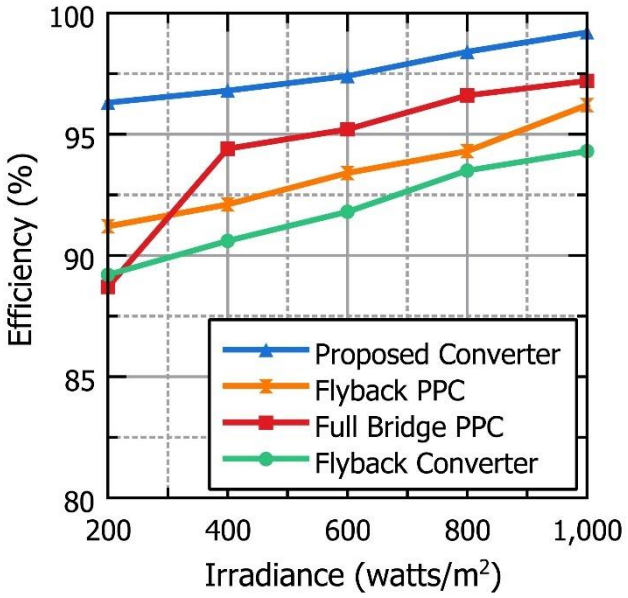

Fig. 10. Efficiency curves of the converter

It is noticed that as the global voltage gain increases, the partial power ratio increases, and the amount of

active power processed decreases. This feature makes the converter work in high efficiency even at low irradiance levels. The output power P_{out} varies, and it maintains the MPP. The average converter efficiency is 99.2% and the amount of power processing done by the converter P_{conv} is only a portion of P_{out}. This helps the converter to maintain the higher efficiency even in the low irradiance levels.

4 Conclusion

In this paper, a series partial power converter using HB LLC topology for PV application is proposed, with high efficiency and faster transient response is proposed. The highly efficient operation achieved by soft-switching features makes HB LLC based S-PPC a very attractive solution for the front-end conversion stage of AC/DC converters. The voltage gain formula of the proposed converter is developed in this paper, and the partial power ratio K_{pr} is confirmed using MATLAB Simulink. The proposed converter is applied with a modified P&O MPPT algorithm for variable frequency to the converter and the settling time of 10 ms with maximum efficiency of 99.2%. In addition, the proposed converter proves better performance in low irradiance level conditions by maintaining primary-side switches in ZVS and secondary-side diodes in ZCS over the entire operating range.

Reference

[1] J. W. Zapata, S. Kouro, G. Carrasco, H. Renaudineau, and T. A. Meynard, "Analysis of Partial Power DC-DC Converters for Two-Stage Photovoltaic Systems," *IEEE J Emerg Sel Top Power Electron*, vol. 7, no. 1, pp. 591–603, Mar. 2019, doi: 10.1109/JESTPE.2018.2842638.

[2] B. M. Alharbi, M. A. Alhomim, and R. A. McCann, "An efficient high voltage gain using two-stage cascaded interleaved boost converter for solar PV system with MPPT technique," *2020 IEEE Power and Energy Society Innovative Smart Grid Technologies Conference, ISGT 2020*, Feb. 2020, doi: 10.1109/ISGT45199.2020.9087720.

[3] M. Shayestegan, "Overview of grid-connected two-stage transformer-less inverter design," *Journal of Modern Power Systems and Clean Energy*, vol. 6, no. 4, pp. 642–655, Jul. 2018, doi: 10.1007/S40565-017-0367-Z.

[4] A. I. M. Ali and H. R. A. Mohamed, "Improved P&O MPPT algorithm with efficient open-circuit voltage estimation for two-stage grid-integrated PV system under realistic solar radiation," *International Journal of Electrical Power & Energy Systems*, vol. 137, p. 107805, May 2022, doi: 10.1016/J.IJEPES.2021.107805.

[5] A. Priyadarshi, P. K. Kar, and S. B. Karanki, "A wide load range ZVS high voltage gain hybrid DC-DC boost converter based on diode-capacitor voltage multiplier circuit," *International Transactions on Electrical Energy Systems*, vol. 30, no. 1, p. e12171, Jan. 2020, doi: 10.1002/2050-7038.12171.

[6] N. G. F. Dos Santos, J. R. R. Zientarski, and M. L. da S. Martins, "A Review of Series-Connected Partial Power Converters for DC–DC Applications," *IEEE J Emerg Sel Top Power Electron*, 2021, doi: 10.1109/JESTPE.2021.3082869.

[7] D. D. Kumar, B. Challa, and P. Ponnambalam, "A Flyback Partial Power Processing Converter based Solar PV Systems Interfacing the Grid," *2019 Innovations in Power and Advanced Computing Technologies, i-PACT 2019*, Mar. 2019, doi: 10.1109/I-PACT44901.2019.8960045.

[8] J. Anzola *et al.*, "Review of Architectures Based on Partial Power Processing for DC-DC Applications," *IEEE Access*, vol. 8, pp. 103405–103418, 2020, doi: 10.1109/ACCESS.2020.2999062.

[9] F. Flores-Bahamonde, H. Renaudineau, S. Rivera, and S. Kouro, "A two stage approach for step-up/down series partial power conversion in PV application with wide range of operation," *Proceedings of the Energy Conversion Congress and Exposition - Asia, ECCE Asia 2021*, pp. 1946–1951, May 2021, doi: 10.1109/ECCE-ASIA49820.2021.9479437.

[10] C. Fei, R. Gadelrab, Q. Li, and F. C. Lee, "High-Frequency Three-Phase Interleaved LLC Resonant Converter with GaN Devices and Integrated Planar Magnetics," *IEEE J Emerg Sel Top Power Electron*, vol. 7, no. 2, pp. 653–663, Jun. 2019, doi: 10.1109/JESTPE.2019.2891317.

[11] Y. Wei, Q. Luo, and A. Mantooth, "Overview of Modulation Strategies for LLC Resonant Converter," *IEEE Trans Power Electron*, vol. 35, no. 10, pp. 10423–10443, Oct. 2020, doi: 10.1109/TPEL.2020.2975392.

[12] T. N. Gücin, M. Biberoğlu, and B. Fincan, "Constant frequency operation of parallel resonant converter for constant-current constant-voltage battery charger applications," *Journal of Modern Power Systems and Clean Energy*, vol. 7, no. 1, pp. 186–199, Jan. 2019, doi: 10.1007/S40565-018-0403-7.

[13] Y. Chen, J. Xu, Y. Gao, L. Lin, J. Cao, and H. Ma, "Analysis and Design of Phase-Shift Pulse-Frequency-Modulated Full-Bridge LCC Resonant Converter," *IEEE Transactions on Industrial Electronics*, vol. 67, no. 2, pp. 1092–1102, Feb. 2020, doi: 10.1109/TIE.2019.2898586.

[14] X. Tan and X. Ruan, "Equivalence Relations of Resonant Tanks: A New Perspective for Selection and Design of Resonant Converters," *IEEE Transactions on Industrial Electronics*, vol. 63, no. 4, pp. 2111–2123, Apr. 2016, doi: 10.1109/TIE.2015.2506151.

[15] Y. Wei, Q. Luo, and A. Mantooth, "Comprehensive Analysis and Design of LLC Resonant Converter With Magnetic Control," *CPSS Transactions on Power Electronics and Applications*, vol. 4, no. 4, Dec. 2019, doi: 10.24295/CPSSTPEA.2019.00025.

[16] Y. Wei, Q. Luo, and A. Mantooth, "A Hybrid Half-bridge LLC Resonant Converter and Phase Shifted Full-bridge Converter for High Step-up Application," *2020 IEEE Workshop on Wide Bandgap Power Devices and Applications in Asia, WiPDA Asia 2020*, Sep. 2020, doi: 10.1109/WIPDAASIA49671.2020.9360292.

[17] N. Altin, S. Ozdemir, and A. Nasiri, "A novel solar PV inverter topology based on an LLC resonant converter," *2019 IEEE Energy Conversion Congress and Exposition, ECCE 2019*, pp. 6734–6740, Sep. 2019, doi: 10.1109/ECCE.2019.8912924.

[18] R. L. Lin and L. H. Huang, "Efficiency Improvement on LLC Resonant Converter Using Integrated LCLC Resonant Transformer," *IEEE Trans Ind Appl*, vol. 54, no. 2, pp. 1756–1764, Mar. 2018, doi: 10.1109/TIA.2017.2771728.

[19] J. Zeng, G. Zhang, S. S. Yu, B. Zhang, and Y. Zhang, "LLC resonant converter topologies and industrial applications - A review," *Chinese Journal of Electrical Engineering*, vol. 6, no. 3, pp. 73–84, Sep. 2020, doi: 10.23919/CJEE.2020.000021.

[20] N. Altin, S. Ozdemir, M. Khayamy, and A. Nasiri, "A Novel Topology for Solar PV Inverter Based on an LLC Resonant Converter With Optimal Frequency and Phase-Shift Control," *IEEE Trans Ind Appl*, vol. 58, no. 4, pp. 5042–5054, 2022, doi: 10.1109/TIA.2022.3163372.

[21] Y. Liang, X. Liu, and S. Lyu, "A phase-shift modulated series resonant converter achieving zero-voltage and zero-current switching for wide output voltage range battery charging applications," *IET Power Electronics*, vol. 15, no. 16, pp. 1894–1908, Dec. 2022, doi: 10.1049/PEL2.12356.

[22] H. Wen, J. Gong, X. Zhao, C. S. Yeh, and J. S. Lai, "Analysis of diode reverse recovery effect on ZVS condition for GaN-Based LLC resonant converter," *IEEE Trans Power Electron*, vol. 34, no. 12, pp. 11952–11963, Dec. 2019, doi: 10.1109/TPEL.2019.2909426.

[23] M. Z. Ramli and Z. Salam, "Performance evaluation of dc power optimizer (DCPO) for photovoltaic (PV) system during partial shading," *Renew Energy*, vol. 139, pp. 1336–1354, Aug. 2019, doi: 10.1016/J.RENENE.2019.02.072.

[24] J. Liu, J. Zhang, T. Q. Zheng, and J. Yang, "A Modified Gain Model and the Corresponding Design Method for an LLC Resonant Converter," *IEEE Trans Power Electron*, vol. 32, no. 9, pp. 6716–6727, Sep. 2017, doi: 10.1109/TPEL.2016.2623418.

Sebin Davis K was born in Thrissur, (KL) India. He obtained his B. Tech in electrical and electronics engineering from Cochin University of Science and Technology (KL) and M. Tech in power electronics from Calicut University (KL), India in 2009 and 2012, respectively. Presently he works in Sahrdaya Engineering College, Thrissur and pursues his Ph.D. in EED Karunya Institute of Technology and Sciences, Coimbatore, India. His area of interest includes power electronics, renewable energy integration to grid.

Varghese Jegathesan received the B.E. and M.E. degrees from Bharathiar University, Coimbatore, India, in 1999 and 2002 and the Ph.D. degree from Anna University, Chennai, India, in 2010. Currently, he is associate professor in the Department of Electrical and Electronics Engineering at Karunya Institute of Technology and Sciences, India. His area of interest includes electric circuits and networks, power electronics, the development of heuristic algorithms for power electronics applications and the application of power electronics to renewable energy.

Received 28 May 2024